Communication

Impaired Expression of GABA Signaling Components in the Alzheimer's Disease Middle Temporal Gyrus

Karan Govindpani [1] , Clinton Turner [1,2], Henry J Waldvogel [1], Richard L M Faull [1] and Andrea Kwakowsky [1,*]

[1] Centre for Brain Research, Department of Anatomy and Medical Imaging, Faculty of Medical and Health Sciences, University of Auckland, Auckland 1023, New Zealand; k.govindpani@auckland.ac.nz (K.G.); ClintonT@adhb.govt.nz (C.T.); h.waldvogel@auckland.ac.nz (H.J.W.); rlm.faull@auckland.ac.nz (R.L.M.F.)

[2] Department of Anatomical Pathology, LabPlus, Auckland City Hospital, Auckland 1023, New Zealand

* Correspondence: a.kwakowsky@auckland.ac.nz; Tel.: +64-9923-9346

check for updates

Abstract: γ-aminobutyric acid (GABA) is the primary inhibitory neurotransmitter, playing a central role in the regulation of cortical excitability and the maintenance of the excitatory/inhibitory (E/I) balance. Several lines of evidence point to a remodeling of the cerebral GABAergic system in Alzheimer's disease (AD), with past studies demonstrating alterations in GABA receptor and transporter expression, GABA synthesizing enzyme activity and focal GABA concentrations in post-mortem tissue. AD is a chronic neurodegenerative disorder with a poorly understood etiology and the temporal cortex is one of the earliest regions in the brain to be affected by AD neurodegeneration. Utilizing NanoString nCounter analysis, we demonstrate here the transcriptional downregulation of several GABA signaling components in the post-mortem human middle temporal gyrus (MTG) in AD, including the $GABA_A$ receptor α_1, α_2, α_3, α_5, β_1, β_2, β_3, δ, γ_2, γ_3, and θ subunits and the $GABA_B$ receptor 2 ($GABA_B$R2) subunit. In addition to this, we note the transcriptional upregulation of the betaine-GABA transporter (BGT1) and GABA transporter 2 (GAT2), and the downregulation of the 67 kDa isoform of glutamate decarboxylase (GAD_{67}), the primary GABA synthesizing enzyme. The functional consequences of these changes require further investigation, but such alterations may underlie disruptions to the E/I balance that are believed to contribute to cognitive decline in AD.

Keywords: Alzheimer's disease; GABA; GABAergic system; GABA receptors; GABA transporters; middle temporal gyrus

1. Introduction

Alzheimer's disease (AD) is a chronic neurodegenerative disorder of old age with a gradual, insidious presentation [1]. While the underlying etiology of the disease is yet to be elucidated, it is classically associated with the appearance of characteristic pathological markers including the deposition of β-amyloid (Aβ) protein as insoluble extracellular plaques and the formation of intracellular neurofibrillary tangles (NFTs) composed of hyperphosphorylated tau protein (p-tau) [2–5]. Early neuropathological changes are mostly confined to the hippocampal formation [6–8], with the particularly prominent loss of excitatory glutamatergic pyramidal neurons and synaptic connections in this region [9–13]. The progression of pathology, including the loss of excitatory connections, follows a stereotyped pattern, with secondary degeneration observed in the temporal cortex in the early stages of pathogenesis [6,14–17]. The depletion of glutamatergic connections and glutamate receptors in these regions contributes significantly to the memory and cognitive deficits characteristic of the clinical condition [18–22]. Normal cognitive function and memory formation within the hippocampus and cortex is reliant on the careful maintenance of a balance between excitatory and inhibitory

signaling [23–26], the disruption of which may cause impairments in synaptic plasticity and network synchronization [27–29]. Indeed, disturbances in network synchronization and oscillatory activity have been widely reported in the AD brain [30–33]. The glutamatergic system is only one of several neurotransmitter systems involved in AD pathogenesis.

It was long thought that the inhibitory γ-aminobutyric acid (GABA) system is relatively unaffected in AD. Several studies have reported the relative preservation of GABAergic interneurons in various brain regions and their apparent resistance to Aβ-induced degeneration [34–37]. However, a large body of evidence now points to a more subtle remodeling of GABAergic circuits in the AD brain, likely progressing with disease stage [38–40]. At the macrostructural level, the pruning of GABAergic terminals has been reported, particularly in the vicinity of Aβ plaques, indicating a synaptic loss of function despite the preservation of GABAergic fibers [41,42]. Such changes likely underlie the pyramidal hyperexcitability observed in AD, contributing to excitatory/inhibitory (E/I) imbalance [27,38,43]. Many early studies also reported alterations in GABA levels, typically a reduction in total neurotransmitter concentration in several regions of the post-mortem AD brain [38,44]. This by itself is perhaps difficult to interpret due to the effect of agonal state changes on GABA levels in the post-mortem brain [45–48]. However, post-mortem studies have also demonstrated alterations in the subunit configurations of $GABA_A$ receptors ($GABA_A$Rs) in the hippocampus and cortex at the transcriptional and protein level, contributing to the remodeling of the system [48–56]. $GABA_A$Rs are ionotropic receptors with multi-subunit structures, most commonly comprising five subunits arranged around a central Cl^- channel [57]. Receptors may be assembled from several potential subunit isoforms, each belonging to one of eight characterized subunit families—α, β, γ, δ, ρ, ε, θ and π [58,59]. $GABA_A$R subunit isoforms are encoded by at least 21 genes, conferring this class of receptors with significant structural heterogeneity [60,61]. The precise subunit configuration of the $GABA_A$R defines its pharmacological and electrical properties and the composition of post-synaptic $GABA_A$Rs shapes the inhibitory post-synaptic response [58,62,63]. The restructuring of $GABA_A$Rs in the AD brain likely points to a more general alteration in the function of the cerebral inhibitory system. The $GABA_B$ receptor ($GABA_B$R) on the other hand is a metabotropic receptor, comprising two distinct subunits termed $GABA_B$ receptor 1 ($GABA_B$R1) and $GABA_B$ receptor 2 ($GABA_B$R2). These receptors are functionally distinct from $GABA_A$Rs, interacting with K^+ channels, Ca^{2+} channels and adenylate cyclase to modulate membrane potential and couple GABA binding to downstream signaling events [64]. The downregulation of $GABA_B$Rs has been previously reported in the superior frontal gyrus in the AD brain [65] and transient upregulation of $GABA_B$R1 has also been observed in the AD hippocampus in the early stages of the disease [66].

GABA transporters (GATs) are involved predominantly in the removal of GABA from the synaptic cleft following neurotransmission. The four main GAT subtypes within the human brain are GABA transporter 1 (GAT1), GABA transporter 2 (GAT2), GABA transporter 3 (GAT3) and the betaine-GABA transporter (BGT1) [67]. GAT expression is likely altered in the AD brain, as reported in a few previous studies [68–70]. We have previously demonstrated differential alterations in GAT expression within the AD superior temporal gyrus (STG) using an immunohistochemical (IHC) approach. We noted a particularly significant upregulation in BGT1 expression concomitant with the downregulation of GAT1 in this region [70]. Expression changes in glutamate decarboxylase (GAD), the primary GABA synthesizing enzyme, have also been reported in the AD prefrontal and temporal cortex [54,71]. Taken together, these results lend further support to the idea of a general inhibitory deficit in the AD brain, affecting multiple molecular mechanisms within the GABA signaling system.

Given the likely contribution of GABAergic dysfunction to E/I imbalances in the AD hippocampus and temporal cortex, it is important to characterize the development of molecular GABAergic deficits in these brain regions. Limon et al. have previously investigated GABAergic changes in human AD temporal cortex homogenates. Using quantitative polymerase chain reaction (qPCR), this group reported the downregulation of $GABA_A$R α_1, α_2, α_5, β_2, β_3, γ_2 and δ subunit mRNA transcripts and the preservation of $GABA_A$R β_1, γ_1 and ρ_1 subunit transcripts [55]. They further confirmed

the downregulation of $GABA_AR$ α_1 and γ_2 subunit protein expression and the preservation of β_1 and γ_1 subunit protein expression using Western blot analysis [55,72]. However, an examination of subregion-dependent alterations in $GABA_AR$ subunit expression within the temporal cortex was not conducted. In our own subsequent IHC analysis of $GABA_AR$ subunit expression in the AD STG, we noted the downregulation of the α_2 and α_5 subunits and the preservation of the α_1, α_3, β_1, β_2, β_3 and γ_2 subunits [56]. These results further underscore the notion that the GABAergic system may be differentially affected in a subregion-specific manner within the AD temporal cortex.

In this study, we sought to extend our investigations into GABA receptor subunit expression changes in AD to the middle temporal gyrus (MTG), with the careful anatomical isolation of this cortical subregion and the precise quantification of mRNA transcripts utilizing NanoString nCounter analysis. We also investigated transcriptional alterations in the GABA transporters, GADs and the GABA-metabolizing enzyme aminobutyric acid transaminase (ABAT) within the AD MTG. GABA transporter expression has not previously been studied within the AD MTG. We demonstrate here the transcriptional downregulation of several $GABA_AR$ and $GABA_BR$ subunits within the MTG in the AD brain, along with the downregulation of GAD_{67} mRNA and the upregulation of GAT2 and BGT1 transcripts.

2. Results

NanoString nCounter analysis revealed the transcriptional downregulation of several GABAergic system components in the human AD MTG compared with age-matched control cases (Figure 1). This was particularly notable for $GABA_AR$ subunit transcripts, with significant transcriptional downregulation of the α_1, α_2, α_3, α_5, β_1, β_2, β_3, δ, γ_2, γ_3, and θ subunits (encoded by the *GABRA1*, *GABRA2*, *GABRA3*, *GABRA5*, *GABRB1*, *GABRB2*, *GABRB3*, *GABRD*, *GABRG2*, *GABRG3* and *GABRQ* genes, respectively). The transcriptional expression of the $GABA_AR$ α_4 subunit (*GABRA4*) was not significantly altered in the AD MTG, but there was a trend toward downregulation. A trend toward transcriptional upregulation was noted in the $GABA_AR$ γ_1 subunit (*GABRG1*), but this was similarly non-significant. The expression of the $GABA_AR$ ε subunit (*GABRE*) was stable in AD cases. Therefore, most $GABA_AR$ subunits appear to be downregulated at the transcriptional level in the AD MTG. The $GABA_AR$ α_6 and π subunit transcripts (*GABRA6* and *GABRP*, respectively) were not detectable above background levels in these human MTG lysates, while the ε and θ subunits were expressed at very low levels. We also noted the transcriptional downregulation of the $GABA_BR2$ subunit (encoded by *GABBR2*), one of the two metabotropic receptor subunits that form the functional $GABA_BR$. The expression of both the R1a and R1b splice variants of the $GABA_BR1$ subunit (respectively GABBR1_1 and GABBR1_2 in Figure 1) remained unaltered. Using fluorescence immunohistochemistry (fIHC) to label formalin-fixed MTG sections from AD and control cases, we demonstrated qualitatively that marked downregulations in α_1, β_2 and β_3 $GABA_AR$ subunits are also perceptible within the grey matter of the AD MTG at the protein level (Figure 2).

The mRNA expression of the two primary synaptic GABA transporters—GAT1 and GAT3 (encoded by *SLC6A1* and *SLC6A11*, respectively)—did not appear to be altered in the AD MTG and vesicular GABA transporter (vGAT) (*SLC32A1*) mRNA expression also remained unaltered. However, we found that both BGT1 and GAT2 transcripts (*SLC6A12* and *SLC6A13*, respectively) were upregulated.

Finally, we noted the transcriptional downregulation of the 67 kDa isoform of the GABA synthesizing enzyme glutamate decarboxylase (GAD_{67}) (encoded by *GAD1*), but not the 65 kDa isoform (GAD_{65}) (encoded by *GAD2*). The transcriptional expression of ABAT (encoded by *ABAT*) was also unaltered in the AD MTG.
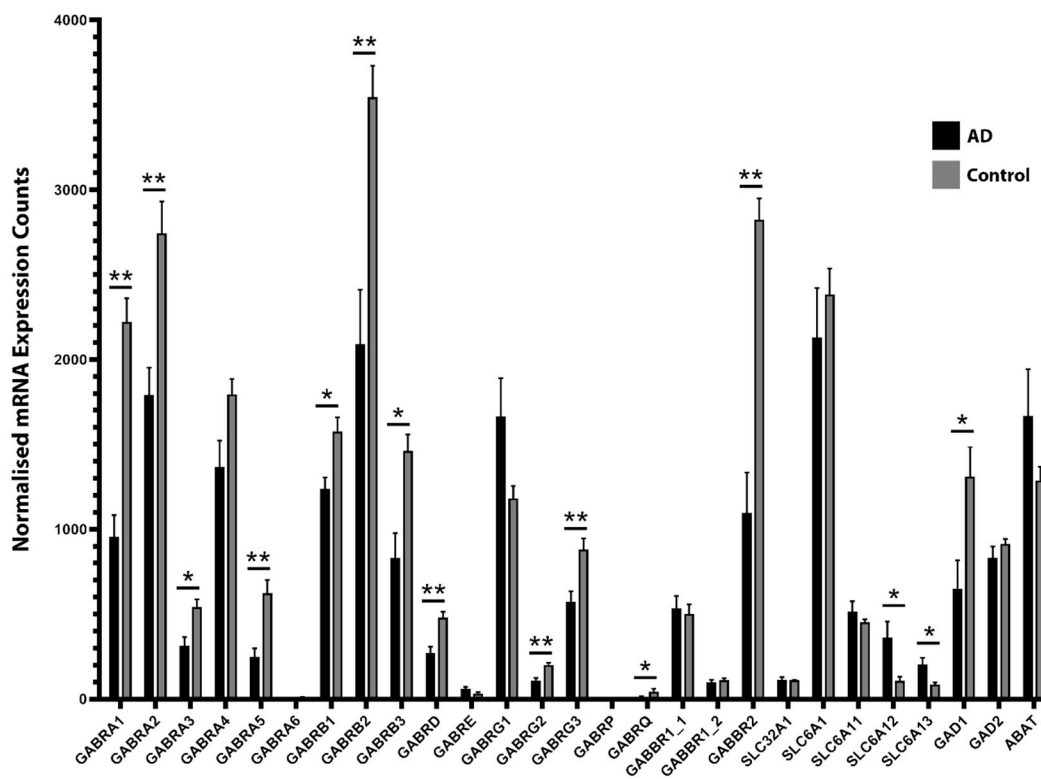
Figure 1. Normalized NanoString nCounter mRNA expression counts for γ-aminobutyric acid (GABA)ergic signaling components in Alzheimer's disease (AD) and control human middle temporal gyrus (MTG) grey matter samples. Several GABAergic signaling components, including $GABA_AR$ subunits, the $GABA_BR2$ subunit, GABA transporters, and the GABA synthesizing enzyme GAD_{67}, are altered in expression in the AD MTG. Raw mRNA counts were normalized to positive control and housekeeping gene counts and background-corrected using negative control counts. For each subunit, normalized mRNA counts were compared between AD and control groups using the Mann–Whitney unpaired test, * $p \leq 0.05$ and ** $p \leq 0.01$. Data presented as mean ± SEM, n = six AD cases and six control cases. Gene names on *x*-axis; GABBR1_1 and GABBR1_2 represent two distinct transcript variants encoded by the *GABBR1* gene.
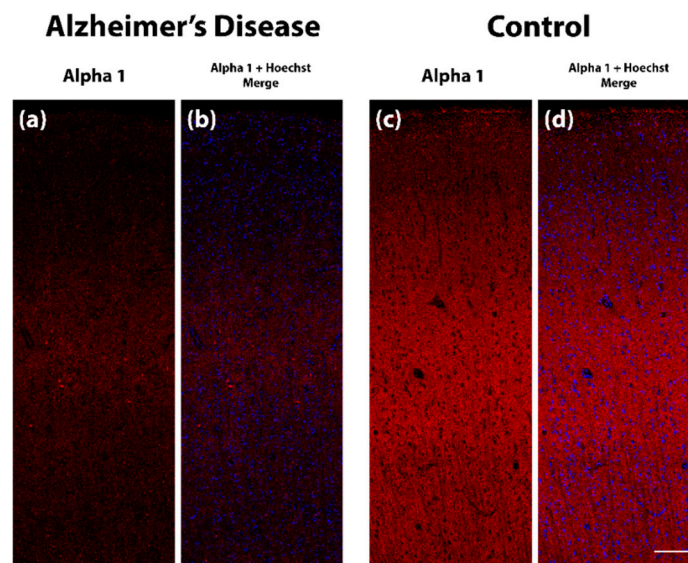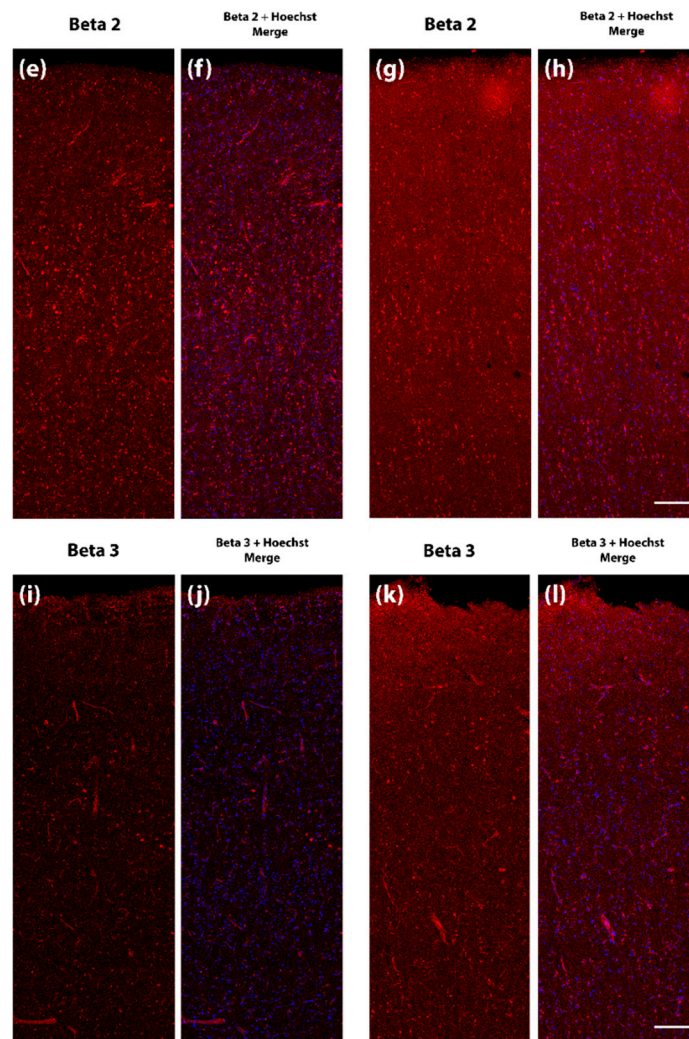

Figure 2. *Cont.*

Figure 2. Representative fluorescent immunohistochemistry images from the human Alzheimer's disease and control middle temporal gyrus (MTG). Post-mortem human MTG sections were labelled with antibodies against GABA$_A$R subunits and imaged with uniform settings for each subunit on a confocal microscope. GABA$_A$R subunits are presented in red and Hoechst staining is presented in blue. A reduction in fluorescent intensity across cortical layers was apparent for the α_1 subunit (cases AZ90 and H122 presented) (**a–d**), β_2 subunit (cases AZ90 and H122 presented) (**e–h**) and β_3 subunit (cases AZ90 and H181 presented) (**i–l**). Scale bar, 200 μm.

3. Discussion

In this study, we have demonstrated, for the first time, the transcriptional downregulation of several GABA$_A$R subunits across a defined region of the MTG in AD. In particular, the α_1, α_2, α_3, α_5, β_1, β_2, β_3, δ, γ_2, γ_3, and θ subunits were downregulated in tissue samples from the AD MTG, while the α_4, γ_1 and ε subunits were preserved. Using fIHC, we demonstrated qualitatively the downregulation of GABA$_A$R α_1, β_2 and β_3 subunits in AD MTG sections, indicating the possibility of a concomitant downregulation in these subunit proteins. While this could indicate a remodeling of GABA$_A$R subunit configurations in the MTG, it may alternatively be indicative of a general downregulation in GABA$_A$Rs or the loss of GABA$_A$R-expressing cells in the MTG in the later stages of AD, given the fact that almost all detectable GABA$_A$R subunits appear to be affected in the same manner. Indeed, given the widespread loss of glutamatergic fibers and terminals within the AD temporal cortex, along with GABAergic terminals [6,14–17,41,42], it is to be expected that there will be a concomitant reduction in GABA$_A$R expression detectable in any given mass of tissue homogenate (or equally in any given volume

of total RNA). However, there were some $GABA_A R$ subunits that did not appear to be significantly downregulated, namely the α_4, γ_1 and ε subunits. Indeed, there was a non-significant trend toward the transcriptional upregulation of the γ_1 subunit. This would logically imply that even if there is some contribution of glutamatergic and GABAergic terminal loss to the overall downregulation that we observe in most $GABA_A R$ subunits, there is a mechanism at play whereby some $GABA_A R$ subunits are spared whereas others are more selectively downregulated. Within the limits of the current study, we cannot say with certainty what mechanism may underlie the relative sparing of some subunits. Indeed, this may be a transcriptional mechanism, or it could simply indicate the relative sparing of a subpopulation of neurons or other cell types expressing specific $GABA_A R$ variants. Given the high expression of the α_4 and ε subunits at extrasynaptic sites, it is also conceivable that these are relatively spared during the targeted degeneration of neuronal terminals. However other prominently extrasynaptic subunits such as α_5 and δ [73] were found to be transcriptionally downregulated in the AD MTG and may perhaps be lost with the degeneration of glutamatergic cell bodies. It is important to note that previous IHC studies have demonstrated $GABA_A R$ subunit downregulation in cortical and hippocampal AD tissue at levels greater than may be explainable purely through cellular degeneration, potentially indicating that there is a transcriptional deficit at play. Mizukami et al. demonstrated using *In Situ* hybridization the downregulation of β_3 subunit mRNA even in regions of the AD hippocampus exhibiting little to no cell loss, while β_2 subunit mRNA was preserved even in regions exhibiting severe pathological changes [53]. Iwakiri et al. actually observed that $\gamma_{1/3}$ subunits (using an antibody recognizing both subunits) were upregulated in the CA1–4 hippocampus and dentate gyrus in AD [48]. We too observed a non-significant trend toward upregulation of the γ_1 subunit transcript in the AD MTG. The transcriptional upregulation of some subunits combined with neuronal and synaptosomal loss may result in the detection of overall stable expression in a given subregion. The sensitivity of any particular $GABA_A R$ subunit to loss within a fixed amount of tissue (or total RNA) is thus likely to be dependent on several factors, including alterations in transcription and protein trafficking, the precise localization of receptors at pre- or post-synaptic terminals or extrasynaptic sites, neuronal subtype-specific expression, and local patterns of glutamatergic and GABAergic neuronal and synaptosomal degeneration. The precise mechanisms underlying these effects remain to be determined, but our results indicate a remodeling of the overall $GABA_A R$ subunit composition in the AD MTG. This points to the alteration of the functional and pharmacological properties of the inhibitory system at large, whether these alterations are primary or secondary to degeneration.

While this is the first study to examine such alterations specifically in the MTG, Limon et al. have previously reported AD-associated $GABA_A R$ subunit expression changes across the temporal cortex [55]. Interestingly, they too reported a trend toward the transcriptional downregulation of several subunits, including α_1, α_2, α_5, β_2, β_3, γ_2 and δ. This supports our observation that the same subunit mRNAs are downregulated within the MTG in particular. Their study, like ours, also noted the sparing of γ_1 and ε subunit mRNA expression, indicating that this is likely uniform across the temporal cortex. However, this group reported the sparing of β_1 and θ subunit mRNA expression, while we noted a downregulation in both. This likely indicates a specific loss of these subunits within the MTG in AD, while this may not be the case across the temporal cortex as a whole. It should also be noted that NanoString nCounter analysis is a more sensitive method of transcript quantification than qPCR, giving us a greater ability to detect more subtle alterations in transcript expression. Howell et al. have reported the preservation of $GABA_A R$ α_5 subunit expression in the AD temporal cortex as a whole, however they had quantified subunit protein expression using autoradiography [74], a generally low-resolution technique. As stated earlier, we have previously observed the downregulation of the $GABA_A R$ α_2 and α_5 subunits in the AD STG, with the preservation of α_1, α_3, β_1, β_2, β_3 and γ_2 subunits [56]. There may therefore be differences in the sensitivity of $GABA_A R$ subunits to AD-associated expression changes within the MTG and STG, pointing to differences in subregional vulnerability within the temporal cortex.

We also observed the transcriptional downregulation of the GABA$_B$R2 subunit in the AD MTG, while the GABA$_B$R1 subunit appeared to be spared. This is the first study to examine alterations in GABA$_B$R subunit expression within the human temporal cortex. It is traditionally considered that the formation of a functional GABA$_B$R necessitates the association of both the GABA$_B$R1 and GABA$_B$R2 subunits, given the presence of an endoplasmic reticulum (ER) retention signal on the GABA$_B$R1 subunit that is masked by association with GABA$_B$R2. The GABA$_B$R2 subunit, on the other hand, contains the orthosteric binding site for GABA [75]. The specific downregulation of the GABA$_B$R2 subunit may indicate the downregulation of surface-expressed GABA$_B$Rs, likely resulting in a reduction in functional inhibition in GABA$_B$R-expressing cells. Given the preservation of GABA$_B$R1 subunit transcripts, there may well be increased ER retention of GABA$_B$R1. There is evidence that GABA$_B$R1 subunits in the ER membrane may have alternative roles, participating in intracellular signaling pathways including the ERK/MAPK pathway [76,77], potentially explaining the differential transcriptional changes in these two metabotropic receptor subunits in the AD MTG. Considering the stability of GABA$_B$R1 expression compared with GABA$_B$R2 expression, it is unlikely that the measured reduction in the latter is purely the result of neuronal or synaptosomal loss.

The functional implication of such a general transcriptional down-regulation in both GABA$_A$R and GABA$_B$R subunits is difficult to determine in isolation. However, these results support the idea that AD is associated with the widespread disruption of functional inhibition in brain, including in the temporal cortex. The remodeling of GABA$_A$R subunit configurations on surviving excitatory neurons in the middle to late stages of AD may have subtle but significant implications for the precise pharmacological control of neuronal inhibition, altering GABA$_A$R channel opening and gating, sensitivity to GABA and other endogenous modulators, and GABA$_B$R coupling to downstream signaling pathways and membrane-bound ion channels. Within any given cortical region, this could have a potentially profound impact on the balance between excitation and inhibition in surviving neuronal networks. Therefore, our understanding of E/I balance disruption in the AD temporal cortex requires a factoring of GABAergic remodeling in addition to the well-characterized glutamatergic degeneration.

In the AD MTG, we did not detect transcriptional changes in the primary synaptic GABA transporters—GAT1 and GAT3. This may indicate the general preservation of GABA clearance mechanisms at the synapse. Two previous studies have investigated temporal cortex GAT1/3 expression using radioligand binding techniques. Simpson et al. reported the loss of binding sites for ^{3}[H]nipecotic acid, a non-specific inhibitor of all GABA transporters except BGT1, in AD temporal cortex samples [68], while Nägga et al. reported the preservation of binding sites for ^{3}[H]tiagabine, a specific inhibitor of GAT1 [69]. However, neither study segregated their data by temporal cortex subregion. Our group has previously used IHC techniques to demonstrate the downregulation of GAT1 in the AD STG, with the sparing of GAT3 expression [70]. The current study is, however, the first to examine alterations in GAT1 and GAT3 mRNA expression specifically in the AD MTG, where these species appear to be well conserved. More interesting was our observation of transcriptional upregulation of BGT1 and GAT2 in this region. We have previously reported the same for BGT1 in the STG using IHC, indicating the potential for a general BGT1 upregulation across the temporal cortex in AD. This is perhaps not altogether surprising. BGT1 is not believed to play a significant role in synaptic GABA uptake, being a low-affinity GABA transporter with relatively slow transport kinetics compared with GAT1/3. However, several recent studies have demonstrated a novel role for astrocytic BGT1 in cytoprotective mechanisms, with significant BGT1 upregulation noted in response to osmotic stress and kainate-induced injury [78–80]. We have ourselves previously demonstrated the upregulation of BGT1 in astrocytes within the STG in AD [70]. Therefore, the transcriptional upregulation of BGT1 that we observe here may potentially represent a similar astrocytic upregulation. The transcriptional upregulation of GAT2 is more cryptic, as the precise physiological role of this transporter in the human brain is unknown. However, GAT2 is reportedly expressed on a subpopulation of blood vessels and may play a role in the maintenance of cortical osmolarity through the transport of the osmolyte taurine out of the brain [81].

Finally, we observed in the AD MTG the transcriptional downregulation of the GAD_{67} isoform of GAD, the GABA synthesizing enzyme, but not the GAD_{65} isoform. Schwab et al. previously reported the opposite expressional pattern in the MTG at the protein level—The downregulation of GAD_{65} expression, as measured by IHC and Western blot analysis, and the preservation of GAD_{67} expression, as measured by Western blot analysis [71]. It should be noted however that their Western blot study employed only two AD and two control cases, so it is difficult to draw firm conclusions on this basis. Reinikainen et al. reported in an early study that GAD activity is preserved in human AD temporal cortex homogenates, suggesting that GAD levels across the temporal cortex are not altered [82]. The transcriptional downregulation of GAD_{67} that we observe in the AD MTG may be specific to this subregion of the temporal cortex. This may account for the numerous reports in the literature of reduced GABA neurotransmitter concentrations in the temporal cortex [36,45,83–86] as the GAD_{67} isoform is predominantly responsible for the synthesis of GABA under basal conditions and accounts for the majority of intracellular cytosolic GABA [87,88]. GAD_{65} is targeted to synaptic terminals and plays a greater role in the synaptic release of GABA [89]. The ABAT enzyme, responsible for GABA catabolism, appears to be transcriptionally preserved in the AD MTG, and in association with GAT1/3 preservation, this may indicate that GABA removal and recycling mechanisms at the synapse are relatively spared in the AD MTG.

The precise effect of these alterations in GABAergic signaling component expression remains to be determined. However, it may be hypothesized that the subregion-specificity of such changes results in differential effects on inhibition in different regions of the temporal cortex at any given stage of AD pathogenesis. This may naturally imply the evolution of subregion-specific differences in the firing characteristics of excitatory neurons in the temporal cortex, dependent on the extent and nature of $GABA_A R$ subunit remodeling. Equally, our observation of a general downregulation in most $GABA_A R$ subunit transcripts and the $GABA_B R1$ subunit in the MTG may indicate a more general reduction in GABAergic inhibitory control, conceivably contributing to glutamatergic hyperexcitability in this subregion. Synaptosomal degeneration at inhibitory synapses, coupled with synaptic GABA receptor loss and/or remodeling, could have a profound effect on overall network characteristics. The precise subregion-specific characterization of molecular changes in the inhibitory system therefore contributes to our understanding of the anatomical evolution of these deficits during AD pathogenesis.

In closing, it is perhaps worth considering the implications of such a widespread $GABA_A R$ remodeling to AD symptomatology and therapy. In the introduction, we briefly mentioned mechanisms that may underlie alterations in pyramidal excitability, including inhibitory synaptosomal loss [41,42] and alterations in tonic $GABA_A R$-mediated inhibition [90,91]. Such alterations are likely to play a significant role in the cognitive and memory deficits inherent in the disease. However, other signs of this E/I dysregulation are also apparent in AD, particularly the high incidence of epileptiform activity, including non-motor seizures in the advanced disease [92]. It is interesting to note that temporal lobe epilepsy (TLE) is also associated with alterations in $GABA_A R$ receptor configurations in the temporal cortex and hippocampus [93–96]. While it is difficult to draw direct parallels between $GABA_A R$ receptor plasticity in the two conditions, it is plausible that subunit remodeling has similar functional consequences in the AD temporal cortex alongside other complex Aβ-induced alterations in inhibitory signaling. Alterations in $GABA_A R$ subunit configurations could also alter the pharmacology of GABAergic drugs prescribed to patients with AD, potentially for the treatment of co-morbid conditions. Indeed, benzodiazepines (BZDs), a common class of anxiolytic drugs targeting $γ_2$ subunit-containing $GABA_A Rs$, are commonly prescribed to AD patients for the treatment of behavioral and psychological symptoms [97]. Subunit remodeling and changes in receptor pharmacology could have implications for BZD efficacy in AD patients, but this has not been adequately studied. Prolonged use of BZDs may itself be associated with increased risk of AD in elderly patients [98] and it is not clear how GABAergic-targeted therapies may affect the molecular evolution of inhibitory deficits in the AD brain. Specific $GABA_A R$ subtypes are now emerging as promising targets in the treatment of cognitive deficits and neuronal loss in AD, including the extrasynaptic $α_5$ subunit-containing receptor [99–102].

Therefore, studies such as ours, elucidating subregional GABA$_A$R subunit alterations in AD, could improve the potential for therapeutic targeting in the future.

4. Materials and Methods

4.1. Post-Mortem Human Brain Tissue Processing

　　　Human brain tissue was obtained with informed consent through a donor program at the Neurological Foundation Human Brain Bank at the University of Auckland. All work with human tissue was conducted with the prior approval of the University of Auckland Human Participants Ethics Committee. Tissue from all human cases used in this study had previously been assessed by a neuropathologist and detailed case histories were taken at the time of donation. Control cases were confirmed to have no history of neurological impairment or evidence of neurodegenerative disorders. The control cases did not display tau or amyloid pathology and all AD cases were classified as Braak stage IV-VI based on NFT pathology [6]. In addition, we only considered AD cases that were categorized as Probable AD or Definite AD, based on the criteria established by the Consortium to Establish a Registry for Alzheimer's Disease (CERAD) [103]. In every case, control or AD, the cause of death was unrelated to brain trauma or neurological disease aside from AD dementia for the relevant disease cases. As far as possible, AD and control cases were matched for age, sex and post-mortem delay. Details of the cases used are presented in Tables 1–4. All tissue was processed following protocols that had been developed and validated previously by our group. In brief, the brain is separated into left and right hemispheres, with the right hemisphere perfused with formalin before freezing and the left hemisphere frozen fresh. Each hemisphere is dissected according to a physical–functional map of the brain, resulting in a series of blocks that reproduce the sub-regional organization of several cortical gyri and subcortical structures. This makes it possible to precisely define a subregion of interest for anatomical or molecular investigation. The full procedure for dissection is provided by Waldvogel, et al. [104].

Table 1. Details of control cases for NanoString nCounter Study.

Case	Age	Sex	PM Delay (h)	Cause of Death	Brain Weight (g)
H122	72	F	9	Emphysema	1230
H123	78	M	7.5	Abdominal aortic aneurysm	1260
H131	73	F	13	Ischaemic heart disease	1210
H164	73	M	13	Ischaemic heart disease	1315
H190	72	F	19	Ruptured myocardial infarction	1264
H202	83	M	14	Abdominal aortic aneurysm	1245

　　　Human brains were transported to the Neurological Foundation Human Brain Bank with minimal post-mortem delay and the left and right hemispheres separated. Once the hemispheres of the brain are separated, the left hemisphere is immediately processed by dissecting into physical–functional blocks. The blocks are flash-frozen with powdered dry ice and stored at −80 °C. These may later be sectioned with a cryostat as required. The blocks to be used were later cut into 60 μm-thick sections using a cryostat and the cortical grey matter was isolated carefully with the use of a scalpel. These grey matter samples were frozen at −80 °C for later RNA isolation. In this manner, MTG tissue from 6 AD and 6 age-matched control cases was collected (Tables 1 and 2).

　　　For free-floating IHC, formalin-fixed tissue was used. After separation, the right hemisphere of the brain was flushed through the carotid, vertebral and anterior cerebral arteries with pH 7.4 phosphate-buffered saline (PBS) containing 1% sodium nitrite, to clear the tissue of blood and induce mild vasodilation. The hemisphere was then perfused in the same manner for 30–45 min with 15% formalin in 0.1 M phosphate buffer, pH 7.4. Following perfusion–fixation, the whole hemisphere

was post-fixed by immersing in the same 15% formalin solution for 6–12 h at room temperature (RT). The tissue was then ready for dissection into blocks. The blocks themselves were immersed in fresh fixative for 24–48 h, transferred into a solution of 20% sucrose in 0.1 M phosphate buffer with 0.1% sodium azide for 2–3 days, and then transferred into a solution of 30% sucrose in 0.1 M phosphate buffer with 0.1% sodium azide for another 2–3 days to cryopreserve the tissue. Finally, the formalin-fixed blocks were snap-frozen on powdered dry ice and stored at −80 °C. The required blocks were later cut into 50 μm sections at −35 °C using the HM 450 sliding microtome (Thermo Fisher, Waltham, MA, USA), and these sections were stored at 4 °C in PBS with 0.1% sodium azide.

Table 2. Details of Alzheimer's disease cases for NanoString nCounter Study.

Case	Age	Sex	PM Delay (h)	Cause of Death	CERAD Class.	Braak Stage Score	Brain Weight (g)
AZ38	80	M	5.5	Pneumonia emphysema	Definite AD	V	1039
AZ45	82	M	4.5	Pneumonia	Probable AD	IV	1200
AZ61	87	F	7.5	Dementia	Definite AD	V	1036
AZ72	70	F	7	Lung cancer	Probable AD	V	1044
AZ90	73	M	4	Gastrointestinal haemorrhage	Definite AD	V	1287
AZ96	74	F	8.5	Metastatic cancer, likely gastric	Definite AD	V	1062

Table 3. Details of control cases for fluorescence immunohistochemistry study.

Case	Age	Sex	PM Delay (h)	Cause of Death	Brain Weight (g)
H122	72	F	9	Emphysema	1230
H123	78	M	7.5	Abdominal aortic aneurysm	1260
H137	77	F	12	Coronary arteriosclerosis	1227
H169	81	M	24	Asphyxia	1225
H180	73	M	33	Ischemic heart disease	1318
H181	78	F	20	Aortic aneurism	1292
H202	83	M	14	Abdominal aortic aneurysm	1245

Table 4. Details of Alzheimer's disease cases for fluorescence immunohistochemistry study.

Case	Age	Sex	PM Delay (h)	Cause of Death	CERAD Class.	Braak Stage Score	Brain Weight (g)
AZ38	80	M	5.5	Pneumonia emphysema	Definite AD	V	1039
AZ45	82	M	4.5	Pneumonia	Probable AD	IV	1200
AZ90	73	M	4	Gastrointestinal haemorrhage	Definite AD	V	1287
AZ92	93	F	11.5	Bronchopneumonia	Probable AD	IV	1123
AZ98	91	F	20.5	Alzheimer's disease/atrial fibrillation	Definite AD	VI	958
AZ102	84	F	14.5	Lower respiratory tract infection	Definite AD	VI	1088
AZ103	87	M	<24	Alzheimer's dementia	Definite AD	IV	1385

4.2. TRIzol RNA Isolation from Fresh-Frozen Human MTG Tissue

RNA isolation from post-mortem tissue was conducted using the RNeasy Lipid Mini Kit (Qiagen, Hilden, Germany, Cat. 74804) using the kit protocol. Tissue samples on dry ice were treated with 1 mL of the QIAzol Lysis Reagent and immediately ground with the use of a pestle followed by syringe homogenization (25-gauge needle). The resulting homogenates were incubated in QIAzol for 5 min at room temperature (RT), after which chloroform was spiked into the homogenate (0.2 mL for every 1 mL of QIAzol). The tubes containing the tissue–QIAzol–chloroform mixture were shaken vigorously for 15 s and incubated for 3 min at RT. Phase separation was achieved by centrifugation at $15,000 \times g$ for 15 min at 4 °C. For each sample, the aqueous phase was carefully separated with a pipette and transferred to a fresh Eppendorf and one volume of ice-cold 70% ethanol was added to each sample. After brief mixing, the mixtures were transferred into RNeasy spin columns and centrifuged at $8000 \times g$ for 15 s. In total, 700 μL of Buffer RW1 was added to each column and they were centrifuged at $8000 \times g$ for a further 15 s. In total, 500 μL of Buffer RPE was washed through the column by centrifuging at $8000 \times g$ for 15 s, and this was repeated a second time. The spin columns were dried by centrifuging at $11,500 \times g$ for 1 min, and then RNA was eluted by adding RNase-free water to the spin columns and centrifuging at $8000 \times g$ for 1 min. RNA sample purity was assessed using the NanoDrop spectrophotometer (Thermo Fisher, Waltham, MA, USA) and RNA integrity was tested with the Agilent 2100 Bioanalyzer (Agilent Technologies, Santa Clara, CA, USA). In all cases, samples displayed DV300 ≥ 60. RIN values ranged from ~5–7 for control tissue and ~4–6 for AD tissue.

4.3. RNA Quantification by NanoString nCounter Analysis

The NanoString nCounter assay was outsourced to The Otago Genomics Facility (University of Otago, Dunedin, New Zealand), and assays were performed as described by Geiss et al. [105]. An nCounter Custom CodeSet library of RNA-specific probes were designed to target transcripts encoded by 26 human genes involved in cerebral GABAergic function and a further 4 housekeeping genes (ACTB, B2M, GAPDH and TOP1) (Table 5). The Custom CodeSet library included both a Capture and Reporter CodeSet specific for each gene of interest. For each gene, probes were designed to hybridize with all known transcript variants, except for *GABBR1*, for which probes were designed to differentially target the R1a and R1b transcript variants.

Briefly, the assay was performed with 100 ng of total RNA per tissue sample. In total, 100 ng total RNA in a 5 μL volume of water was mixed with 3 μL of Reporter CodeSet, 2 μL of Capture CodeSet and 5 μL of hybridization buffer. The hybridization mixture was incubated at 65 °C for 21 h in a thermal cycler. Samples were then loaded onto nCounter Prep Plates for purification before being loaded into nCounter Cartridges for immobilization. Cartridges were quantified using the GEN2 Digital Analyzer (NanoString Technologies, Seattle, WA, USA), a multi-channel epifluorescence scanner for nCounter cartridges, and the "max" field-of-view option selected (555 images per sample). Reporter signals were thus counted across all 555 images. Raw counts per lane were saved to a Reporter Code Count (RCC) file.

Statistical analysis and quality control were conducted using the nSolver Software v.4 (NanoString Technologies, Seattle, WA, USA). A Reporter Library File (RLF) specifying the identities of reporter probe signals was loaded into nSolver, along with the RCC file. Prior to normalization, the mean of raw negative control counts for each sample (8 internal negative control RNA sequences) was subtracted from target counts using nSolver; this was done to prevent comparisons being made for targets that were not actually expressed above background levels in the MTG. Raw counts for all samples and targets were normalized to the geometric mean of averaged raw counts for the 6 positive controls across the same samples. CodeSet content normalization was conducted to determine sample-specific correction factors for all counts for each individual sample; this is based on a normalization to the geometric mean of housekeeping gene average raw counts for each sample. This normalization procedure produces a single compound normalization factor for counts from each sample, allowing raw data to be corrected for technical variability in assay procedure. In addition, for each sample,

the raw counts of the 8 internal negative control RNA sequences were manually normalized using the same compound normalization factor that had been applied by nSolver to target raw counts for that sample.

Table 5. Complete list of genes, isoform accession numbers and target sequences for NanoString nCounter probes.

HUGO Gene	Gene Name	Accession Number(s)
ABAT	GABA transaminase	NM_001127448.1; NM_020686.5; NM_000663.4
ACTB *	Beta-actin	NM_001101.3
B2M *	Beta-2-microglobulin	NM_004048.2
GABBR1	$GABA_B$ receptor 1 subunit, isoform a	NM_001470.3
GABBR1	$GABA_B$ receptor 1 subunit, isoform b	NM_021903.2
GABBR2	$GABA_B$ receptor 2 subunit	NM_005458.7
GABRA1	$GABA_A$ receptor α_1 subunit	NM_001127643.1; NM_000806.5; NM_001127648.1; NM_001127645.1; NM_001127644.1 NM_001330690.1;
GABRA2	$GABA_A$ receptor α_2 subunit	NM_001114175.2; NM_001286827.2; NM_000807.3
GABRA3	$GABA_A$ receptor α_3 subunit	NM_000808.3
GABRA4	$GABA_A$ receptor α_4 subunit	NM_001204266.1; NM_001204267.1; NM_000809.3
GABRA5	$GABA_A$ receptor α_5 subunit	NM_000810.3; NM_001165037.1
GABRA6	$GABA_A$ receptor α_6 subunit	NM_000811.2
GABRB1	$GABA_A$ receptor β_1 subunit	NM_000812.3
GABRB2	$GABA_A$ receptor β_2 subunit	NM_021911.2; NM_000813.2
GABRB3	$GABA_A$ receptor β_3 subunit	NM_001278631.1; NM_000814.5; NM_001191320.1; NM_021912.4; NM_001191321.2
GABRD	$GABA_A$ receptor δ subunit	NM_000815.4
GABRE	$GABA_A$ receptor ε subunit	NM_004961.3
GABRG1	$GABA_A$ receptor γ_1 subunit	NM_173536.3
GABRG2	$GABA_A$ receptor γ_2 subunit	NM_198903.2; NM_000816.3; NM_198904.2
GABRG3	$GABA_A$ receptor γ_3 subunit	NM_033223.4; NM_001270873.1
GABRP	$GABA_A$ receptor π subunit	NM_001291985.1; NM_014211.2
GABRQ	$GABA_A$ receptor θ subunit	NM_018558.3
GAD1	Glutamic acid decarboxylase, 67 kDa isoform	NM_000817.2
GAD2	Glutamic acid decarboxylase, 65 kDa isoform	NM_000818.2; NM_001134366.1
GAPDH *	Glyceraldehyde-3-phosphate dehydrogenase	NM_001256799.2; NM_001289746.1; NM_001289745.1; NM_002046.5
SLC32A1	Vesicular GABA transporter (vGAT)	NM_080552.2
SLC6A1	GABA transporter 1 (GAT1)	NM_003042.3
SLC6A11	GABA transporter (GAT3)	NM_001317406.1; NM_014229.2
SLC6A12	Betaine transporter 1 (BGT1)	NM_001206931.1; NM_003044.4; NM_001122847.2; NM_001122848.2
SLC6A13	GABA transporter 2 (GAT2)	NM_001190997.2; NM_001243392.1; NM_016615.4
TOP1 *	DNA topoisomerase 1	NM_003286.3

* Housekeeping genes.

To determine whether normalized mRNA counts for each target differed significantly between AD and control MTG tissue, normalized counts from 6 AD and 6 control cases were compared using the Mann–Whitney unpaired test. RNA target expression was considered to be altered if there was a statistically significant difference between normalized counts for each group ($p \leq 0.05$). A non-parametric test was used as data did not meet the assumptions of a parametric test, i.e., normality and homogeneity of variance.

4.4. Free-Floating Fluorescence Immunohistochemistry (fIHC)

Seven control and 7 AD cases were stained to assess GABA$_A$R subunit expression (Tables 3 and 4). Two MTG sections per case were washed overnight with PBS supplemented with 0.2% Triton X-100 (PBST). Following this, sections were washed with PBST a further three times for 10 min and treated with primary antibodies raised against the GABA$_A$R α_1 subunit (mouse monoclonal, clone BD24, gifted by Jean-Marc Fritschy, Switzerland; 1:5000), β_2 subunit (rabbit polyclonal, Novus, NBP1-51214; 1:1000) or β_3 subunit (mouse monoclonal, Novus, NBP1-47613; 1:1000) for 72 h at 4 °C. All antibodies were diluted in an immunobuffer consisting of 1% normal goat serum and 0.04% *w/v* merthiolate in PBST. Sections were washed with PBST three times for 10 min and then treated with the appropriate Alexa Fluor goat secondary antibodies (Anti-Rabbit IgG Fluor 647, Thermo Fisher, A21245; Anti-Mouse IgG Alexa Fluor 647, Thermo Fisher, A21236) diluted 1:500 in immunobuffer for 24 h at RT. Sections were washed once with PBST and treated with Hoechst 33,342 (Molecular Probes, H-3570; 1:1000). Sections were washed three times in PBS and were then mounted onto glass microscopy slides with Mowiol-488 mounting medium and coverslipped with #1.5 glass coverslides. Fluorescent imaging was conducted using the LSM710 laser-scanning inverted confocal microscope (Carl Zeiss AG, Oberkochen, Germany). A 2×6 tile-scan image was taken for each section encompassing all layers of the cortex. AD and control sections stained for each GABA$_A$R subunit were imaged at the same settings to ensure comparability and analysed qualitatively.

Author Contributions: K.G. and A.K. performed the research and analysed the data; K.G., H.J.W., R.L.M.F. and A.K. wrote the paper and designed the study; C.T. carried out the pathology for all human brain tissue; K.G., R.L.M.F. and A.K. were responsible for the funding acquisition; A.K. was responsible for project administration; H.J.W., R.L.M.F. and A.K. supervised the study. All authors have read and agreed to the published version of the manuscript.

Abbreviations

Aβ	Amyloid-beta
ABAT	4-aminobutyrate aminotransferase
AD	Alzheimer's disease
BGT1	Betaine-GABA transporter 1
BZD	Benzodiazepine
CA	Cornu Ammonis
CERAD	Consortium to Establish a Registry for Alzheimer's Disease
E/I	Excitatory/Inhibitory
ER	Endoplasmic reticulum
fIHC	Fluorescence immunohistochemistry

GABA	Gamma-aminobutyric acid
GABA$_A$R	GABA$_A$ receptor
GABA$_B$R	GABA$_B$ receptor
GABA$_B$R1	GABA$_B$ receptor subunit 1
GABA$_B$R2	GABA$_B$ receptor subunit 2
GAD	Glutamate decarboxylase
GAD$_{65}$	Glutamate decarboxylase, 65 kDa isoform
GAD$_{67}$	Glutamate decarboxylase, 67 kDa isoform
GAT	GABA transporter
GAT1	GABA transporter 1
GAT2	GABA transporter 2
GAT3	GABA transporter 3
IgG	Immunoglobulin G
IHC	Immunohistochemistry
MTG	Middle temporal gyrus
NFT	Neurofibrillary tangle
PBS	Phosphate-buffered saline
PM	Post-mortem
p-tau	Phosphorylated tau protein
qPCR	Quantitative polymerase chain reaction
RCC	Reporter code count
RLF	Reporter library file
RNA	Ribonucleic acid
RT	Room temperature
STG	Superior temporal gyrus
TLE	Temporal lobe epilepsy
vGAT	Vesicular GABA transporter

References

1. McKhann, G.M.; Knopman, D.S.; Chertkow, H.; Hyman, B.T.; Jack, C.R., Jr.; Kawas, C.H.; Klunk, W.E.; Koroshetz, W.J.; Manly, J.J.; Mayeux, R.; et al. The diagnosis of dementia due to Alzheimer's disease: Recommendations from the National Institute on Aging-Alzheimer's Association workgroups on diagnostic guidelines for Alzheimer's disease. *Alzheimer's Dement.* **2011**, *7*, 263–269. [CrossRef] [PubMed]

2. Grundke-Iqbal, I.; Iqbal, K.; Tung, Y.C.; Quinlan, M.; Wisniewski, H.M.; Binder, L.I. Abnormal phosphorylation of the microtubule-associated protein tau (tau) in Alzheimer cytoskeletal pathology. *Proc. Natl. Acad. Sci. USA* **1986**, *83*, 4913–4917. [CrossRef] [PubMed]

3. Beyreuther, K.; Masters, C.L. Nomenclature of amyloid A4 proteins and their precursors in Alzheimer's disease and down's syndrome. *Neurobiol. Aging* **1990**, *11*, 66–68. [CrossRef]

4. Hardy, J.A.; Higgins, G.A. Alzheimer's disease: The amyloid cascade hypothesis. *Science* **1992**, *256*, 184–185. [CrossRef] [PubMed]

5. Chen, X.-Q.; Mobley, W.C. Alzheimer disease pathogenesis: Insights from molecular and cellular biology studies of oligomeric Aβ and tau species. *Front. Neurosci.* **2019**, *13*, 659. [CrossRef]

6. Braak, H.; Braak, E. Neuropathological stageing of Alzheimer-related changes. *Acta Neuropathol.* **1991**, *82*, 239–259. [CrossRef]

7. Scahill, R.I.; Schott, J.M.; Stevens, J.M.; Rossor, M.N.; Fox, N.C. Mapping the evolution of regional atrophy in Alzheimer's disease: Unbiased analysis of fluid-registered serial MRI. *Proc. Natl. Acad. Sci. USA* **2002**, *99*, 4703–4707. [CrossRef]

8. Zakzanis, K.K.; Graham, S.J.; Campbell, Z. A meta-analysis of structural and functional brain imaging in dementia of the Alzheimer's type: A neuroimaging profile. *Neuropsychol. Rev.* **2003**, *13*, 1–18. [CrossRef]

9. Davies, D.C.; Horwood, N.; Isaacs, S.L.; Mann, D.M.A. The effect of age and Alzheimer's disease on pyramidal neuron density in the individual fields of the hippocampal formation. *Acta Neuropathol.* **1992**, *83*, 510–517. [CrossRef]

10. Doebler, J.A.; Markesbery, W.R.; Anthony, A.; Rhoads, R.E. Neuronal RNA in relation to neuronal loss and neurofibrillary pathology in the hippocampus in Alzheimer's disease. *J. Neuropathol. Exp. Neurol.* **1987**, *46*, 28–39. [CrossRef]

11. Rössler, M.; Zarski, R.; Bohl, J. Stage-dependent and sector-specific neuronal loss in hippocampus during Alzheimer's disease. *Acta Neuropathol.* **2002**, *103*, 363–369. [CrossRef]

12. Mann, D.M.A.; Yates, P.O.; Marcyniuk, B. Some morphometric observations on the cerebral cortex and hippocampus in presenile Alzheimer's disease, senile dementia of Alzheimer type and Down's syndrome in middle age. *J. Neurol. Sci.* **1985**, *69*, 139–159. [CrossRef]

13. Ball, M.J. Neuronal loss, neurofibrillary tangles and granulovacuolar degeneration in the hippocampus with ageing and dementia. A quantitative study. *Acta Neuropathol.* **1977**, *37*, 111–118. [CrossRef] [PubMed]

14. Pearson, R.C.; Esiri, M.M.; Hiorns, R.W.; Wilcock, G.K.; Powell, T.P. Anatomical correlates of the distribution of the pathological changes in the neocortex in Alzheimer disease. *Proc. Natl. Acad. Sci. USA* **1985**, *82*, 4531–4534. [CrossRef] [PubMed]

15. Berron, D.; van Westen, D.; Ossenkoppele, R.; Strandberg, O.; Hansson, O. Medial temporal lobe connectivity and its associations with cognition in early Alzheimer's disease. *Brain* **2020**, *143*, 1233–1248. [CrossRef] [PubMed]

16. Scheff, S.W.; Price, D.A.; Schmitt, F.A.; Scheff, M.A.; Mufson, E.J. Synaptic loss in the inferior temporal gyrus in mild cognitive impairment and Alzheimer's disease. *J. Alzheimer's Dis.* **2011**, *24*, 547–557. [CrossRef] [PubMed]

17. Khan, U.A.; Liu, L.; Provenzano, F.A.; Berman, D.E.; Profaci, C.P.; Sloan, R.; Mayeux, R.; Duff, K.E.; Small, S.A. Molecular drivers and cortical spread of lateral entorhinal cortex dysfunction in preclinical Alzheimer's disease. *Nat. Neurosci.* **2014**, *17*, 304–311. [CrossRef]

18. Terry, R.D.; Masliah, E.; Salmon, D.P.; Butters, N.; DeTeresa, R.; Hill, R.; Hansen, L.A.; Katzman, R. Physical basis of cognitive alterations in alzheimer's disease: Synapse loss is the major correlate of cognitive impairment. *Ann. Neurol.* **1991**, *30*, 572–580. [CrossRef]

19. Kravitz, E.; Gaisler-Salomon, I.; Biegon, A. Hippocampal glutamate NMDA receptor loss tracks progression in Alzheimer's disease: Quantitative autoradiography in postmortem human brain. *PLoS ONE* **2013**, *8*, e81244. [CrossRef]

20. Elgh, E.; Åstot, A.L.; Fagerlund, M.; Eriksson, S.; Olsson, T.; Näsman, B. Cognitive dysfunction, hippocampal atrophy and glucocorticoid feedback in Alzheimer's disease. *Biol. Psychiatry* **2006**, *59*, 155–161. [CrossRef]

21. Hyman, B.T.; Van Hoesen, G.W.; Damasio, A.R.; Barnes, C.L. Alzheimer's disease: Cell-specific pathology isolates the hippocampal formation. *Science* **1984**, *225*, 1168–1170. [CrossRef] [PubMed]

22. Yang, X.; Yao, C.; Tian, T.; Li, X.; Yan, H.; Wu, J.; Li, H.; Pei, L.; Liu, D.; Tian, Q.; et al. A novel mechanism of memory loss in Alzheimer's disease mice via the degeneration of entorhinal–CA1 synapses. *Mol. Psychiatry* **2018**, *23*, 199–210. [CrossRef] [PubMed]

23. Boyce, R.; Glasgow, S.D.; Williams, S.; Adamantidis, A. Causal evidence for the role of REM sleep theta rhythm in contextual memory consolidation. *Science* **2016**, *352*, 812–816. [CrossRef] [PubMed]

24. Huh, C.Y.L.; Amilhon, B.; Ferguson, K.A.; Manseau, F.; Torres-Platas, S.G.; Peach, J.P.; Scodras, S.; Mechawar, N.; Skinner, F.K.; Williams, S. Excitatory inputs determine phase-locking strength and spike-timing of ca1 stratum oriens/alveus parvalbumin and somatostatin interneurons during intrinsically generated hippocampal theta rhythm. *J. Neurosci.* **2016**, *36*, 6605–6622. [CrossRef] [PubMed]

25. Froemke, R.C. Plasticity of cortical excitatory-inhibitory balance. *Annu. Rev. Neurosci.* **2015**, *38*, 195–219. [CrossRef] [PubMed]

26. Amilhon, B.; Huh, C.Y.L.; Manseau, F.; Ducharme, G.; Nichol, H.; Adamantidis, A.; Williams, S. Parvalbumin interneurons of hippocampus tune population activity at theta frequency. *Neuron* **2015**, *86*, 1277–1289. [CrossRef] [PubMed]

27. Busche, M.A.; Konnerth, A. Impairments of neural circuit function in Alzheimer's disease. *Philos. Trans. R. Soc. Lond. B Biol. Sci.* **2016**, *371*, 20150429. [CrossRef]

28. Selten, M.; van Bokhoven, H.; Nadif Kasri, N. Inhibitory control of the excitatory/inhibitory balance in psychiatric disorders. *F1000Research* **2018**, *7*, 23. [CrossRef]

29. Varela, E.V.; Etter, G.; Williams, S. Excitatory-inhibitory imbalance in Alzheimer's disease and therapeutic significance. *Neurobiol. Dis.* **2019**, *127*, 605–615. [CrossRef]

30. Osipova, D.; Ahveninen, J.; Jensen, O.; Ylikoski, A.; Pekkonen, E. Altered generation of spontaneous oscillations in Alzheimer's disease. *NeuroImage* **2005**, *27*, 835–841. [CrossRef]

31. Palop, J.J.; Mucke, L. Network abnormalities and interneuron dysfunction in Alzheimer disease. *Nat. Rev. Neurosci.* **2016**, *17*, 777–792. [CrossRef] [PubMed]

32. Palop, J.J.; Chin, J.; Roberson, E.D.; Wang, J.; Thwin, M.T.; Bien-Ly, N.; Yoo, J.; Ho, K.O.; Yu, G.-Q.; Kreitzer, A.; et al. Aberrant excitatory neuronal activity and compensatory remodeling of inhibitory hippocampal circuits in mouse models of Alzheimer's disease. *Neuron* **2007**, *55*, 697–711. [CrossRef] [PubMed]

33. de Waal, H.; Stam, C.J.; de Haan, W.; van Straaten, E.C.W.; Scheltens, P.; van der Flier, W.M. Young Alzheimer patients show distinct regional changes of oscillatory brain dynamics. *Neurobiol. Aging* **2012**, *33*, 1008.e1025–1008.e1031. [CrossRef] [PubMed]

34. Pike, C.J.; Cotman, C.W. Cultured GABA-immunoreactive neurons are resistant to toxicity induced by β-amyloid. *Neuroscience* **1993**, *56*, 269–274. [CrossRef]

35. Hof, P.R.; Nimchinsky, E.A.; Celio, M.R.; Bouras, C.; Morrison, J.H. Calretinin-immunoreactive neocortical interneurons are unaffected in Alzheimer's disease. *Neurosci. Lett.* **1993**, *152*, 145–149. [CrossRef]

36. Rossor, M.N.; Garrett, N.J.; Johnson, A.L.; Mountjoy, C.Q.; Roth, M.; Iversen, L.L. A post-mortem study of the cholinergic and GABA systems in senile dementia. *Brain* **1982**, *105*, 313–330. [CrossRef]

37. Bell, K.F.S.; Ducatenzeiler, A.; Ribeiro-da-Silva, A.; Duff, K.; Bennett, D.A.; Claudio Cuello, A. The amyloid pathology progresses in a neurotransmitter-specific manner. *Neurobiol. Aging* **2006**, *27*, 1644–1657. [CrossRef]

38. Govindpani, K.; Calvo-Flores Guzmán, B.; Vinnakota, C.; Waldvogel, H.J.; Faull, R.L.; Kwakowsky, A. Towards a Better Understanding of GABAergic Remodeling in Alzheimer's Disease. *Int. J. Mol. Sci.* **2017**, *18*, 1813. [CrossRef]

39. Villette, V.; Dutar, P. GABAergic Microcircuits in Alzheimer's Disease Models. *Curr. Alzheimer Res.* **2017**, *14*, 30–39. [CrossRef]

40. Kwakowsky, A.; Calvo-Flores Guzmán, B.; Govindpani, K.; Waldvogel, H.J.; Faull, R.L. Gamma-aminobutyric acid A receptors in Alzheimer's disease: Highly localized remodeling of a complex and diverse signaling pathway. *Neural Regen. Res.* **2018**, *13*, 1362–1363. [CrossRef]

41. Garcia-Marin, V.; Blazquez-Llorca, L.; Rodriguez, J.-R.; Boluda, S.; Muntane, G.; Ferrer, I.; DeFelipe, J. Diminished perisomatic GABAergic terminals on cortical neurons adjacent to amyloid plaques. *Front. Neuroanat.* **2009**, *3*, 28. [CrossRef] [PubMed]

42. Hardy, J.; Cowburn, R.; Barton, A.; Reynolds, G.; Dodd, P.; Wester, P.; O'Carroll, A.M.; Lofdahl, E.; Winblad, B. A disorder of cortical GABAergic innervation in Alzheimer's disease. *Neurosci. Lett.* **1987**, *73*, 192–196. [CrossRef]

43. Bi, D.; Wen, L.; Wu, Z.; Shen, Y. GABAergic dysfunction in excitatory and inhibitory (E/I) imbalance drives the pathogenesis of Alzheimer's disease. *Alzheimer's Dement.* **2020**, *16*, 1312–1329. [CrossRef] [PubMed]

44. Xu, Y.; Zhao, M.; Han, Y.; Zhang, H. GABAergic inhibitory interneuron deficits in Alzheimer's disease: Implications for treatment. *Front. Neurosci.* **2020**, *14*, 660. [CrossRef] [PubMed]

45. Lowe, S.L.; Francis, P.T.; Procter, A.W.; Palmer, A.M.; Davison, A.N.; Bowen, D.M. Gamma-aminobutyric acid concentration in brain tissue at two stages of Alzheimer's disease. *Brain* **1988**, *111*, 785–799. [CrossRef]

46. Erdő, S.L. Postmortem increase of GABA levels in peripheral rat tissues: Prevention by 3-mercapto-propionic acid. *J. Neural Trans.* **1984**, *60*, 303–314. [CrossRef] [PubMed]

47. Perry, T.L.; Hansen, S.; Gandham, S.S. Postmortem changes of amino compounds in human and rat brain. *J. Neurochem.* **1981**, *36*, 406–410. [CrossRef] [PubMed]

48. Iwakiri, M.; Mizukami, K.; Ikonomovic, M.D.; Ishikawa, M.; Abrahamson, E.E.; DeKosky, S.T.; Asada, T. An immunohistochemical study of GABA$_A$ receptor gamma subunits in Alzheimer's disease hippocampus: Relationship to neurofibrillary tangle progression. *Neuropathology* **2009**, *29*, 263–269. [CrossRef]

49. Mizukami, K.; Ikonomovic, M.D.; Grayson, D.R.; Sheffield, R.; Armstrong, D.M. Immunohistochemical study of GABA$_A$ receptor α1 subunit in the hippocampal formation of aged brains with Alzheimer-related neuropathologic changes. *Brain Res.* **1998**, *799*, 148–155. [CrossRef]

50. Rissman, R.A.; Mishizen-Eberz, A.J.; Carter, T.L.; Wolfe, B.B.; De Blas, A.L.; Miralles, C.P.; Ikonomovic, M.D.; Armstrong, D.M. Biochemical analysis of GABA$_A$ receptor subunits α1, α5, β1, β2 in the hippocampus of patients with Alzheimer's disease neuropathology. *Neuroscience* **2003**, *120*, 695–704. [CrossRef]

51. Rissman, R.A.; Bennett, D.A.; Armstrong, D.M. Subregional analysis of GABAA receptor subunit mRNAs in the hippocampus of older persons with and without cognitive impairment. *J. Chem. Neuroanat.* **2004**, *28*, 17–25. [CrossRef] [PubMed]

52. Mizukami, K.; Ikonomovic, M.D.; Grayson, D.R.; Rubin, R.T.; Warde, D.; Sheffield, R.; Hamilton, R.L.; Davies, P.; Armstrong, D.M. Immunohistochemical study of GABA$_A$ receptor β2/3 subunits in the hippocampal formation of aged brains with Alzheimer-related neuropathologic changes. *Exp. Neurol.* **1997**, *147*, 333–345. [CrossRef]

53. Mizukami, K.; Grayson, D.R.; Ikonomovic, M.D.; Sheffield, R.; Armstrong, D.M. GABA$_A$ receptor β2 and β3 subunits mRNA in the hippocampal formation of aged human brain with Alzheimer-related neuropathology. *Mol. Brain Res.* **1998**, *56*, 268–272. [CrossRef]

54. Luchetti, S.; Bossers, K.; Van de Bilt, S.; Agrapart, V.; Morales, R.R.; Frajese, G.V.; Swaab, D.F. Neurosteroid biosynthetic pathways changes in prefrontal cortex in Alzheimer's disease. *Neurobiol. Aging* **2011**, *32*, 1964–1976. [CrossRef] [PubMed]

55. Limon, A.; Reyes-Ruiz, J.M.; Miledi, R. Loss of functional GABA$_A$ receptors in the Alzheimer diseased brain. *Proc. Natl. Acad. Sci. USA* **2012**, *109*, 10071–10076. [CrossRef] [PubMed]

56. Kwakowsky, A.; Calvo-Flores Guzmán, B.; Pandya, M.; Turner, C.; Waldvogel, H.J.; Faull, R.L. GABA$_A$ receptor subunit expression changes in the human Alzheimer's disease hippocampus, subiculum, entorhinal cortex and superior temporal gyrus. *J. Neurochem.* **2018**, *145*, 374–392. [CrossRef]

57. Nayeem, N.; Green, T.P.; Martin, I.L.; Barnard, E.A. Quaternary structure of the native GABA$_A$ receptor determined by electron microscopic image analysis. *J. Neurochem.* **1994**, *62*, 815–818. [CrossRef]

58. Barnard, E.A.; Skolnick, P.; Olsen, R.W.; Mohler, H.; Sieghart, W.; Biggio, G.; Braestrup, C.; Bateson, A.N.; Langer, S.Z. International Union of Pharmacology. XV. Subtypes of γ-aminobutyric acid$_A$ receptors: Classification on the basis of subunit structure and receptor function. *Pharmacol. Rev.* **1998**, *50*, 291–314.

59. Bonnert, T.P.; McKernan, R.M.; Farrar, S.; le Bourdellès, B.; Heavens, R.P.; Smith, D.W.; Hewson, L.; Rigby, M.R.; Sirinathsinghji, D.J.S.; Brown, N.; et al. θ, a novel γ-aminobutyric acid type A receptor subunit. *Proc. Natl. Acad. Sci. USA* **1999**, *96*, 9891–9896. [CrossRef]

60. Macdonald, R.L.; Olsen, R.W. GABA$_A$ Receptor Channels. *Ann. Rev. Neurosci.* **1994**, *17*, 569–602. [CrossRef]

61. Simon, J.; Wakimoto, H.; Fujita, N.; Lalande, M.; Barnard, E.A. Analysis of the set of GABA$_A$ receptor genes in the human genome. *J. Biol. Chem.* **2004**, *279*, 41422–41435. [CrossRef] [PubMed]

62. Rudolph, U.; Möhler, H. Analysis of GABA$_A$ receptor function and dissection of the pharmacology of benzodiazepines and general anesthetics through mouse genetics. *Ann. Rev. Pharmacol. Toxicol.* **2004**, *44*, 475–498. [CrossRef] [PubMed]

63. Verdoorn, T.A.; Draguhn, A.; Ymer, S.; Seeburg, P.H.; Sakmann, B. Functional properties of recombinant rat GABA$_A$ receptors depend upon subunit composition. *Neuron* **1990**, *4*, 919–928. [CrossRef]

64. Padgett, C.L.; Slesinger, P.A. GABA$_B$ receptor coupling to G-proteins and ion channels. *Adv. Pharmacol.* **2010**, *58*, 123–147. [CrossRef] [PubMed]

65. Chu, D.C.M.; Penney, J.B.; Young, A.B. Cortical GABA$_B$ and GABA$_A$ receptors in Alzheimer's disease. *A Quantitative Autoradiographic Study. Neurology* **1987**, *37*, 1454. [CrossRef] [PubMed]

66. Iwakiri, M.; Mizukami, K.; Ikonomovic, M.D.; Ishikawa, M.; Hidaka, S.; Abrahamson, E.E.; DeKosky, S.T.; Asada, T. Changes in hippocampal GABA$_B$R1 subunit expression in Alzheimer's patients: Association with Braak staging. *Acta Neuropathol.* **2005**, *109*, 467–474. [CrossRef] [PubMed]

67. Scimemi, A. Structure, function, and plasticity of GABA transporters. *Front. Cell. Neurosci.* **2014**, *8*, 161. [CrossRef]

68. Simpson, M.D.C.; Cross, A.J.; Slater, P.; Deakin, J.F.W. Loss of cortical GABA uptake sites in Alzheimer's disease. *J. Neural Trans.* **1988**, *71*, 219–226. [CrossRef]

69. Nägga, K.; Bogdanovic, N.; Marcusson, J. GABA transporters (GAT-1) in Alzheimer's disease. *J. Neural Trans.* **1999**, *106*, 1141–1149. [CrossRef]

70. Fuhrer, T.E.; Palpagama, T.H.; Waldvogel, H.J.; Synek, B.J.L.; Turner, C.; Faull, R.L.; Kwakowsky, A. Impaired expression of GABA transporters in the human Alzheimer's disease hippocampus, subiculum, entorhinal cortex and superior temporal gyrus. *Neuroscience* **2017**, *351*, 108–118. [CrossRef]

71. Schwab, C.; Yu, S.; Wong, W.; McGeer, E.G.; McGeer, P.L. GAD65, GAD67, and GABAT immunostaining in human brain and apparent GAD65 loss in Alzheimer's disease. *J. Alzheimer's Dis.* **2013**, *33*, 1073–1088. [CrossRef] [PubMed]

72. Bernareggi, A.; Dueñas, Z.; Reyes-Ruiz, J.M.; Ruzzier, F.; Miledi, R. Properties of glutamate receptors of Alzheimer's disease brain transplanted to frog oocytes. *Proc. Natl. Acad. Sci. USA* **2007**, *104*, 2956–2960. [CrossRef] [PubMed]

73. Sieghart, W.; Sperk, G. Subunit composition, distribution and function of GABA$_A$ receptor subtypes. *Curr. Top. Med. Chem.* **2002**, *2*, 795–816. [CrossRef] [PubMed]

74. Howell, O.; Atack, J.R.; Dewar, D.; McKernan, R.M.; Sur, C. Density and pharmacology of α5 subunit-containing GABA$_A$ receptors are preserved in hippocampus of Alzheimer's disease patients. *Neuroscience* **2000**, *98*, 669–675. [CrossRef]

75. Galvez, T.; Duthey, B.; Kniazeff, J.; Blahos, J.; Rovelli, G.; Bettler, B.; Prézeau, L.; Pin, J.-P. Allosteric interactions between GB1 and GB2 subunits are required for optimal GABA$_B$ receptor function. *EMBO J.* **2001**, *20*, 2152–2159. [CrossRef]

76. Baloucoune, G.A.; Chun, L.; Zhang, W.; Xu, C.; Huang, S.; Sun, Q.; Wang, Y.; Tu, H.; Liu, J. GABA$_B$ receptor subunit GB1 at the cell surface independently activates ERK1/2 through IGF-1R transactivation. *PLoS ONE* **2012**, *7*, e39698. [CrossRef]

77. Richer, M.; David, M.; Villeneuve, L.R.; Trieu, P.; Ethier, N.; Pétrin, D.; Mamarbachi, A.M.; Hébert, T.E. GABA-B$_1$ receptors are coupled to the ERK1/2 MAP kinase pathway in the absence of GABA-B$_2$ subunits. *J. Mol. Neurosci.* **2009**, *38*, 67–79. [CrossRef]

78. Bitoun, M.; Tappaz, M. Gene expression of the transporters and biosynthetic enzymes of the osmolytes in astrocyte primary cultures exposed to hyperosmotic conditions. *Glia* **2000**, *32*, 165–176. [CrossRef]

79. Olsen, M.; Sarup, A.; Larsson, O.M.; Schousboe, A. Effect of hyperosmotic conditions on the expression of the betaine-GABA-transporter (BGT-1) in cultured mouse astrocytes. *Neurochem. Res.* **2005**, *30*, 855–865. [CrossRef]

80. Zhu, X.M.; Ong, W.Y. Changes in GABA transporters in the rat hippocampus after kainate-induced neuronal injury: Decrease in GAT-1 and GAT-3 but upregulation of betaine/GABA transporter BGT-1. *J. Neurosci. Res.* **2004**, *77*, 402–409. [CrossRef]

81. Zhou, Y.; Holmseth, S.; Guo, C.; Hassel, B.; Höfner, G.; Huitfeldt, H.S.; Wanner, K.T.; Danbolt, N.C. Deletion of the γ-aminobutyric acid transporter 2 (GAT2 and SLC6A13) gene in mice leads to changes in liver and brain taurine contents. *J. Biol. Chem.* **2012**, *287*, 35733–35746. [CrossRef] [PubMed]

82. Reinikainen, K.J.; Paljärvi, L.; Huuskonen, M.; Soininen, H.; Laakso, M.; Riekkinen, P.J. A post-mortem study of noradrenergic, serotonergic and GABAergic neurons in Alzheimer's disease. *J. Neurol. Sci.* **1988**, *84*, 101–116. [CrossRef]

83. Rossor, M.N.; Iversen, L.L.; Reynolds, G.P.; Mountjoy, C.Q.; Roth, M. Neurochemical characteristics of early and late onset types of Alzheimer's disease. *Br. Med. J. (Clin. Res. Ed.)* **1984**, *288*, 961–964. [CrossRef] [PubMed]

84. Ellison, D.W.; Beal, M.F.; Mazurek, M.F.; Bird, E.D.; Martin, J.B. A postmortem study of amino acid neurotransmitters in Alzheimer's disease. *Ann. Neurol.* **1986**, *20*, 616–621. [CrossRef]

85. Seidl, R.; Cairns, N.; Singewald, N.; Kaehler, S.T.; Lubec, G. Differences between GABA levels in Alzheimer's disease and Down syndrome with Alzheimer-like neuropathology. *Naunyn Schmiedeberg's Arch. Pharmacol.* **2001**, *363*, 139–145. [CrossRef]

86. Sasaki, H.; Muramoto, O.; Kanazawa, I.; Arai, H.; Kosaka, K.; Iizuka, R. Regional distribution of amino acid transmitters in postmortem brains of presenile and senile dementia of Alzheimer type. *Ann. Neurolog.* **1986**, *19*, 263–269. [CrossRef]

87. Asada, H.; Kawamura, Y.; Maruyama, K.; Kume, H.; Ding, R.; Ji, F.Y.; Kanbara, N.; Kuzume, H.; Sanbo, M.; Yagi, T.; et al. Mice lacking the 65 kDa isoform of glutamic acid decarboxylase (GAD65) maintain normal levels of GAD67 and GABA in their brains but are susceptible to seizures. *Biochem. Biophys. Res. Commun.* **1996**, *229*, 891–895. [CrossRef]

88. Asada, H.; Kawamura, Y.; Maruyama, K.; Kume, H.; Ding, R.-G.; Kanbara, N.; Kuzume, H.; Sanbo, M.; Yagi, T.; Obata, K. Cleft palate and decreased brain γ-aminobutyric acid in mice lacking the 67-kDa isoform of glutamic acid decarboxylase. *Proc. Natl. Acad. Sci. USA* **1997**, *94*, 6496–6499. [CrossRef]

89. Tian, N.; Petersen, C.; Kash, S.; Baekkeskov, S.; Copenhagen, D.; Nicoll, R. The role of the synthetic enzyme GAD65 in the control of neuronal γ-aminobutyric acid release. *Proc. Natl. Acad. Sci. USA* **1999**, *96*, 12911–12916. [CrossRef]

90. Calvo-Flores Guzmán, B.; Kim, S.; Chawdhary, B.; Peppercorn, K.; Tate, W.P.; Waldvogel, H.J.; Faull, R.L.; Montgomery, J.; Kwakowsky, A. Amyloid-Beta(1-42)-induced increase in GABAergic tonic conductance in mouse hippocampal CA1 pyramidal cells. *Molecules* **2020**, *25*, 693. [CrossRef]

91. Wu, Z.; Guo, Z.; Gearing, M.; Chen, G. Tonic inhibition in dentate gyrus impairs long-term potentiation and memory in an Alzheimer's disease model. *Nat. Commun.* **2014**, *5*, 4159. [CrossRef] [PubMed]

92. Vossel, K.A.; Tartaglia, M.C.; Nygaard, H.B.; Zeman, A.Z.; Miller, B.L. Epileptic activity in Alzheimer's disease: Causes and clinical relevance. *Lancet Neurol.* **2017**, *16*, 311–322. [CrossRef]

93. Loup, F.; Wieser, H.G.; Yonekawa, Y.; Aguzzi, A.; Fritschy, J.M. Selective alterations in GABA_A receptor subtypes in human temporal lobe epilepsy. *J. Neurosci.* **2000**, *20*, 5401–5419. [CrossRef] [PubMed]

94. Rocha, L.; Alonso-Vanegas, M.; Martínez-Juárez, I.E.; Orozco-Suárez, S.; Escalante-Santiago, D.; Feria-Romero, I.A.; Zavala-Tecuapetla, C.; Cisneros-Franco, J.M.; Buentello-García, R.M.; Cienfuegos, J. GABAergic alterations in neocortex of patients with pharmacoresistant temporal lobe epilepsy can explain the comorbidity of anxiety and depression: The potential impact of clinical factors. *Front. Cell. Neurosci.* **2015**, *8*, 442. [CrossRef] [PubMed]

95. Loup, F.; Picard, F.; André, V.M.; Kehrli, P.; Yonekawa, Y.; Wieser, H.-G.; Fritschy, J.-M.J.B. Altered expression of α3-containing GABA_A receptors in the neocortex of patients with focal epilepsy. *Brain* **2006**, *129*, 3277–3289. [CrossRef]

96. Pirker, S.; Schwarzer, C.; Czech, T.; Baumgartner, C.; Pockberger, H.; Maier, H.; Hauer, B.; Sieghart, W.; Furtinger, S.; Sperk, G. Increased expression of GABA_A receptor β-subunits in the hippocampus of patients with temporal lobe epilepsy. *J. Neuropathol. Exp. Neurol.* **2003**, *62*, 820–834. [CrossRef] [PubMed]

97. Defrancesco, M.; Marksteiner, J.; Fleischhacker, W.W.; Blasko, I. Use of benzodiazepines in Alzheimer's disease: A systematic review of literature. *Int. J. Neuropsychopharmacol.* **2015**, *18*, pyv055. [CrossRef]

98. Islam, M.M.; Iqbal, U.; Walther, B.; Atique, S.; Dubey, N.K.; Nguyen, P.A.; Poly, T.N.; Masud, J.H.B.; Li, Y.C.; Shabbir, S.A. Benzodiazepine use and risk of dementia in the elderly population: A systematic review and meta-analysis. *Neuroepidemiology* **2016**, *47*, 181–191. [CrossRef]

99. Vinnakota, C.; Govindpani, K.; Tate, W.P.; Peppercorn, K.; Anekal, P.V.; Waldvogel, H.J.; Faull, R.L.M.; Kwakowsky, A. An α5 GABAA receptor inverse agonist, α5IA, attenuates amyloid beta-induced neuronal death in mouse hippocampal cultures. *Int. J. Mol. Sci.* **2020**, *21*, 3284. [CrossRef]

100. Jacob, T.C. Neurobiology and therapeutic potential of α5-GABA type A receptors. *Front. Mol. Neurosci.* **2019**, *12*, 179. [CrossRef]

101. Dawson, G.R.; Maubach, K.A.; Collinson, N.; Cobain, M.; Everitt, B.J.; MacLeod, A.M.; Choudhury, H.I.; McDonald, L.M.; Pillai, G.; Rycroft, W.; et al. An inverse agonist selective for alpha5 subunit-containing GABAA receptors enhances cognition. *J. Pharmacol. Exp. Ther.* **2006**, *316*, 1335–1345. [CrossRef] [PubMed]

102. Chambers, M.S.; Atack, J.R.; Carling, R.W.; Collinson, N.; Cook, S.M.; Dawson, G.R.; Ferris, P.; Hobbs, S.C.; O'Connor, D.; Marshall, G.; et al. An orally bioavailable, functionally selective inverse agonist at the benzodiazepine site of GABA_A alpha5 receptors with cognition enhancing properties. *J. Med. Chem.* **2004**, *47*, 5829–5832. [CrossRef] [PubMed]

103. Mirra, S.S.; Heyman, A.; McKeel, D.; Sumi, S.M.; Crain, B.J.; Brownlee, L.M.; Vogel, F.S.; Hughes, J.P.; van Belle, G.; Berg, L. The Consortium to Establish a Registry for Alzheimer's Disease (CERAD). Part II. Standardization of the neuropathologic assessment of Alzheimer's disease. *Neurology* **1991**, *41*, 479–486. [CrossRef] [PubMed]

104. Waldvogel, H.J.; Curtis, M.A.; Baer, K.; Rees, M.I.; Faull, R.L.M. Immunohistochemical staining of post-mortem adult human brain sections. *Nat. Protoc.* **2006**, *1*, 2719–2732. [CrossRef]

105. Geiss, G.K.; Bumgarner, R.E.; Birditt, B.; Dahl, T.; Dowidar, N.; Dunaway, D.L.; Fell, H.P.; Ferree, S.; George, R.D.; Grogan, T.; et al. Direct multiplexed measurement of gene expression with color-coded probe pairs. *Nat. Biotech.* **2008**, *26*, 317–325. [CrossRef]

Publisher's Note: MDPI stays neutral with regard to jurisdictional claims in published maps and institutional affiliations.